SIGNIFICANCE

RNA lies at the center of cellular function. Its most recognized role is to carry protein blueprints to the ribosome for manufacture. Only recently have researchers begun to appreciate its myriad of other functions, many of which also lie at the center of important cellular processes and are implicated in a variety of disease states [1, 11, 12]. Long noncoding RNA (lncRNA) comprise one such important class of RNA that does not participate in the central dogma [13]. Alarmingly, the human genome encodes for as many lncRNA as proteins [13, 14]. These transcripts are typically greater than 200 bases, and participate in binding both proteins and nucleic acids, often at the same time [12, 13]. In a striking example, *SNHG5* is a long noncoding RNA (lncRNA) of largely unknown function that that has been linked to cancer cell survival and metastasis in a diversity of cancers from leukemias to melanoma [15–22]. This 2 kilobase transcript localizes to the cytoplasm and is upregulated in these disease states. *SNHG5* has been implicated to interact with a variety of mRNAs to control expression, though little else is known about its role in normal cell function. Where and when does *SNHG5*, and other similar lncRNA, interact with their mRNA targets? How long do these interactions occur, and what other cellular machinery is present? Despite such burning questions in the field of lncRNA, a tool to directly image these species and their interacting partners in living cells has yet to be reported. *Herein, I propose a robust imaging tool for multicomponent, single-molecule visualization of RNA dynamics in living cells.*

BACKGROUND

Protein studies benefit from a large imaging toolkit that has been developed over the last 25 years. Genetically encodable fluorescent proteins are now ubiquitous for studying the localization of any translated target in the cell. While fluorescent proteins are a mature, well-understood technology, tools for imaging the localization of individual RNA transcripts in living cells remain limited. The most popular systems to date include dye-binding aptamers (Spinach [6], Broccoli [7], and Mango [8, 9]), and RNA-binding protein fusions (MS2-FPs) [10, 23].

The most analogous to fluoresecent proteins, dye-binding aptamers utilize exogenously administered dyes that give fluorescence induction upon binding their RNA partner [6–9, 24, 25]. This sequence is encoded downstream of an RNA of interest to track its location in the cell. Though excellent binders for their dyes, these aptamers are unstable in mammalian cells due to their nonnative structure [3, 26–28]. Additionally, though fluorescence turn-on is excellent *in vitro* (often reaching 1,000 fold) signal induction in cells is typically greatly reduced (two to four fold), most likely due to nonspecific binding of the dye. This reduces sensitivity and makes fluorogenic aptamers poor probes for single-molecule tracking [8].

RNA-binding protein fusions are a much more robust technique for imaging individual RNA transcripts [10]. This method often utilizes the MS2 bacteriophage coat protein that binds an encoded stem loop of RNA. When MS2 is fused to a fluorescent protein, transcripts containing the stem loop binding partner can be visualized in the cell. In order to concentrate the fluorescence signal above background, multiple loops are placed in series (up to 24 in a row). Though this technique has enabled imaging of single transcripts in the cell [10, 29], the resulting protein-RNA complex is prohibitively large for many studies, often reaching more than 2,000 kilodaltons [23].

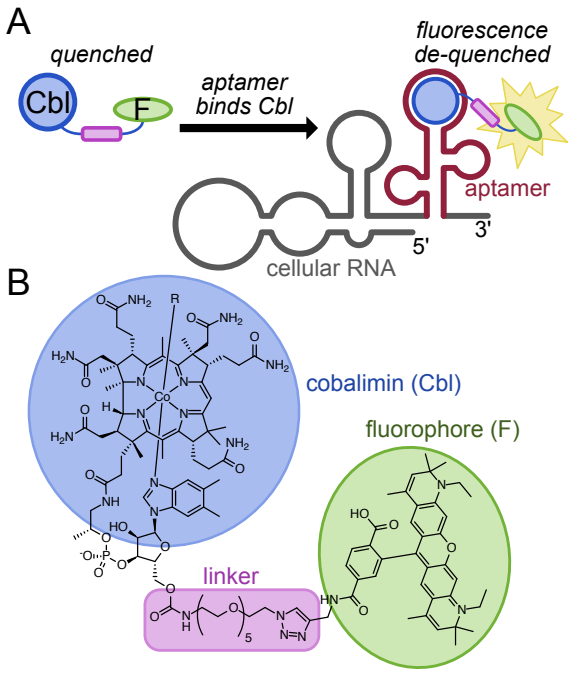

Figure 1. A) Cobalamin acts as a quenching and localization moiety to guide a fluorescent probe to an RNA transcript of interest. When unbound, fluorescence is quenched. In the presence of RNA tagged with the cobalamin riboswitch, fluorescence is restored. B) Structure of the generation 1 Riboglow probe. A polyethylene glycol linker of five units (5xPEG) connected to the 5' hydroxly of the cobalamin ribose was used to tether an ATTO 590 fluorophore to the construct.

Riboglow is a recently developed platform in the Palmer lab that improves on both the size and sensitivity of current RNA imaging techniques (Figure 1) [4]. The two-component system utilizes a synthetic fluorophore-quencher pair (Figure 1B), and a genetically-encoded riboswitch. A transcript of interest is first tagged within the cell, and the probe is administered via bead loading [29–31]. When the construct binds the transcribed riboswitch, the fluorophore is dequenched, giving fluorescent signal (Figure 1A). Riboglow utilizes a riboswitch receptor domain that natively binds a vitamin B_{12} small molecule (cobalamin, Cbl, Figure 1B) [5]. Conveniently, cobalamin is known to act as a fluorescence quencher for a variety of fluorophores [32–34]. With Riboglow, the cobalamin center is conjugated to the fluorophore through a flexible linker that promotes quenching in the unbound state, but enables the fluorophore to reside at a distance in the bound state (Figure 1B).

The Palmer lab found that this initial generation of Riboglow has the potential to outperform existing tools in the field. Its use of a naturally-occurring riboswitch imparts stability to the construct that is not present in aptamer-based techniques [35]. Additionally, the use of a donor-quencher pair reduces nonspecific fluorescence in the unbound state, *providing up to a seven-fold turn-on that significantly increases sensitivity*. With the aptamer-binding dyes, such signal induction is low *(two to four fold)*, and cannot be obtained at all with the MS2-fluorescent protein fusions. *Finally, Riboglow is 10-100 times smaller than the existing techniques and is thus less perturbing to cellular functions.* Due to these advantages, Riboglow outperformed Broccoli and the MS2 system in initial studies of mRNA stress granule (SG) localization in mammalian cells [4].

Though promising, the initial iteration of Riboglow has significant room for improvement. Signal induction upon riboswitch binding never exceeded seven fold *in vitro*, and the pendant dye was not fully quenched (with 10-20% residual fluorescence), *causing significant background signal* [4]. Additionally, to effectively detect stress granules, four riboswitches had to be placed in series to concentrate fluorescence signal [4], *and 12 had to be used to detect single mRNA transcipts (unpublished)*. Thus, the high background precluded single-molecule imaging *without a very bulky probe*. Finally, the strategy cannot currently be used to monitor the location of multiple transcripts in tandem. Herein, I will propose strategies to overcome these limitations through simultaneous modulation of the small molecule construct and riboswitch sequence. *Because 12 copies of Riboglow are currently required to image a single RNA, I will target a 12 fold improvement in the Riboglow system (Aims 1 and 2).* First, I will synthesize a variety of new Riboglow probes to improve fluorescence quenching and lower background fluorescence (Aim 1). Next, A screen for brightness will select the best riboswitch sequence to match the optimized cobalamin probe, *further improving sensitivity* (Aim 2). This new, brighter pair will be tested for single-molecule detection. Finally, I will use SELEX to identify mutually orthogonal probe-riboswitch pairs for multicomponent RNA imaging, and will test these new tools by tracking lncRNA-mRNA interactions in living cells (Aim 3).

APPROACH Aim 1. Synthesize improved Riboglow probes.

The main drawback of Riboglow is the poor turn-on upon probe binding *which limits the sensitivity of the technique by raising fluorescence background*. In this aim, I intend to leverage my background in synthetic chemistry to produce a panel of diverse probe structures that improve fluorescence quenching (and thus signal induction). In previous studies in collaboration with Professor Dorota Gryko (see Gryko letter of support) a small number of linkers and fluorophores were evaluated for quenching and fluorescence turn-on. Linker length and fluorophore wavelength were varied to gauge the quenching ability of cobalamin. Remarkably, some degree of quenching occurred in all of the constructs synthesized, regardless of the spectral overlap of the fluorophore and the cobalamin. However, most retained 10-20% residual fluorescence, which increased background signal significantly. *To optimize probe function, I will vary linker composition, attachment point, and pendant fluorophore with the goal of obtaining 2% residual fluorescence in vitro.*

Ideally, in the unbound state, the cobalamin and fluorophore would be closely associated to maximize FRET and contact quenching [32, 38, 39]. In the RNA-bound state, the molecules would reside at their maximal distance to promote fluorescence [33]. To strike this balance, I will use a synthetic β-hairpin as the linker between cobalamin and the fluorophore (Figure 2B, Table 1). A number of such β-hairpins have been developed, and are referred to as tryptophan zippers [40]. These motifs are as small as twelve amino acids and some are stable

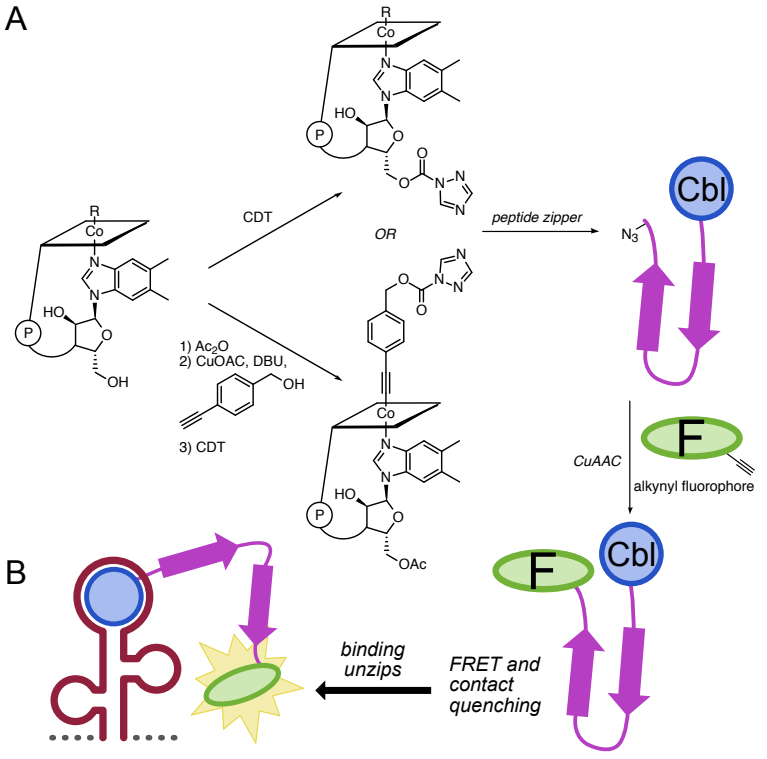

Figure 2. A) Synthesis of two structurally distinct attachment points for Riboglow probes. Both modes of conjugation have already been described in Ref. [36] (see Gryko support letter). Top: Conjugation with CDT at the ribose 5' OH was used in the first-generation probes [4]. Bottom: Alkynylation at the metal center with 4-ethynylbenzyl alcohol will enable subsequent coupling with CDT. Ac_2O: acetic anhydride, DBU: 1,8-diazabicyclo[5.4.0]undec-7-ene, CDT: 1,1-carbonyl-di-(1,2,4-triazole), CuAAC: copper catalyzed azide-alkyne cycloaddition. B) Tryptophan zipper peptides will be used to maximize FRET and contact quenching in the unbound state.

to denaturation up to 85 °C (Table 1). In the unbound state, such a linker would hold the quencher and fluorophore in close proximity (due to the short distance between the N and C-termini of the peptide, Figure 2B). When the cobalamin is bound by the riboswitch, steric occlusion would force the β-hairpin to unfold and place the fluorophore-quencher pair at a larger distance. A wide range of tryptophan zippers have been developed with a variety of structures and stabilities, enabling easy construction of a range of different linkers via solid phase peptide synthesis [37, 40–42] (see Equipment document). To enable modularity, an azidoalanine amino acid will be appended to the C-termini of all linkers during peptide synthesis. Cobalamin will then be coupled to the linker via amide coupling and alkynyl fluorphores will be appended via copper catalyzed azide-alkyne cycloaddition (CuAAC, Figure 2A) [43, 44]. This general synthetic sequence is very similar to that used to make the original Riboglow probes [4]. A starting set if linkers are listed in Table 1. The polyglycine linker will be used as a negative control for a sequence with little secondary structure, but identical length. If the zipper folds prove to be too stable (dequenching is not observed), the amino acids will be varied to tune the melting temperature. Or, if adequate quenching is not observed, the relative positions of the N and C-termini will be adjusted based upon structural data available in the Protein Data Bank (PDB) [42]. All newly synthesized Riboglow probes will be purified via high-performance liquid chromatography (HPLC), and structurally verified via nuclear magnetic resonance (NMR) spectroscopy and high resolution mass spectrometry (HRMS). Each new construct will be tested for its ability to quench fluorescence in vitro by comparing the fluorescence of the construct with that of the free fluorophore in solution. Fluorescence signal in the presence of the Riboglow riboswitch will also be measured to calculate fluorescence turn-on.

Sequence	Tm (°C)	% folded (25 °C)
KKWTW-NPATGK-WTWQE(Az)	85	>96
KKYTW-NPATGK-WTVQE(Az)	66	92
GEWTY-NPATGK-FTVTE(Az)	47	74
GGGGG-GGGGGG-GGGGG(Az)	N/A	N/A

Table 1. Tryptophan zippers of varying stability will be tested to maximize fluorescence quenching. Azidoalanine (Az) will be added to the C-terminus to enable easy fluorophore conjugation. Values were obtained from ref. [37] and reflect measurements for the peptide without the C-terminal azidoalanine.

Another underexplored variable of the original Riboglow probes is the linker attachment point. Though the 5' hydroxyl of the cobalamin ribose is the most accessible nucleophile on the structure, there exist several other possible sites of conjugation. Perhaps the second most common site is the axial ligand of the cobalt metal. Though many studies have taken advantage of the labile nature of certain alkyl modifications at this position [38], others have found alkynyl modifications to be stable to air and light [45, 46]. Following this precedent, I will synthesize a cobalamin with an alkyne handle attached to the cobalt metal center (Figure 2A, Bottom). Such a molecule has already been synthesized in the lab of Professor Dorota Gryko (see Gryko letter of support), and shown to be amenable to functionalization [36].

These constructs will also be evaluated for degree of fluorescence quenching, and brightness in the presence and absence of the cobalamin riboswitch. It is possible that incorporation of a ligand at this site on the metal center will abolish binding to the native riboswitch due to its positioning in the binding pocket [5]. If this is the case, these probes could serve as excellent starting points for directed evolution of orthogonal aptamer-probe pairs (see Aim 3). Additionally, perturbations to the native binding mode of cobalamin could reduce off-target association with native B_{12} machinery [47], further reducing fluorescence background.

The final variable in the molecular structure of the Riboglow probe is the fluorophore itself. *New fluorophores will be explored to maximize quenching in the unbound state.* Additionally, the ideal probe would exhibit minimal cellular autofluorescence by using a red fluorophore with a high extinction coefficient. The Janelia Fluor series of dyes is well suited for this application [48, 49]. With minor modifications to the rhodamine scaffold, Janelia Fluors have varying excitation and emission spectra, and excellent photophysical properties. Table 2 includes a subset of the probes that will be explored. Emphasis will be placed on fluorophores with high extinction coefficients (ϵ) and quantum yields (ϕ), with the intent for these probes to be used in single-molecule imaging (Aim 2). Additionally, JF_{585} and JF_{635} were shown to be highly fluorogenic upon conjugation to a protein tag, with absorbance increases of 80 and 113-fold respectively [48]. The Lavis lab makes these

Dye	λ_{ex} (nm)	λ_{em} (nm)	ϵ ($M^{-1}cm^{-1}$)	ϕ
Cy5	646	662	271,000	0.2
ATTO 488	501	523	90,000	0.8
ATTO 590	594	624	120,000	0.8
ATTO 633	629	657	130,000	0.6
JF_{549}	**549**	**571**	**101,000**	**0.88**
JF_{585}	**585**	**609**	**156,000**	**0.78**
JF_{635}	**635**	**652**	**167,000**	**0.56**

Table 2. A range of fluorophores will be explored for optimal quenching and signal induction. Cy5 and the ATTO series were utilized in the first generation Riboglow system, and will also be used here with new linkers and Cbl attachment points. Photophysical values were obtained from Atto tec and refs. [4] and [48]. λ: wavelength, ϵ: extinction coefficient, ϕ: quantum yield.

probes freely available, and has offered (personal communication) to provide us with alkynylated versions for easy conjugation via CuAAC (Figure 2A). Probes containing these new fluorophores will be evaluated for fluorescence quenching as previously described, with the addition of a test of fluorophore photostability (important for single-molecule imaging, Aim 2).

Expected Outcomes and alternate approaches:
To identify probes with improved quenching and fluorescence turn-on, linker, attachment point, and fluorophore will be varied. To start, I will target a reduction to 2% residual fluorescence *in vitro*. With four linkers, two attachment points, and seven fluorophores, 56 constructs are possible. Though not all of these will be evaluated, simple chemistries involving amide bond couplings and click chemistry will enable us to sample a large amount of this structure space in a rapid fashion. If β-hairpin zippers do not yield improvements in quenching, other linkers with varying rigidity and lengths will be explored [33], specifically those that promote direct contact between the fluorophore and the cobalamin. Also, it should be noted that new cobalamin constructs are not necessary for the success of aims 2 or 3. It is likely that all three aims will be pursued in parallel, with new discoveries in each informing project direction.

Aim 2. Adapt Riboglow for single-molecule imaging.
Visualization of the lifecycle of single RNA transcripts as they move throughout the cell remains a holy grail of RNA imaging [50]. This is an entirely feasible goal due to the fact that so few copies of an individual RNA transcript exist in a cell at any given time (the samples are by definition sparsely populated) [50–52]. Though several recent studies have demonstrated visualization of individual mRNA transcripts in living cells, all have required the use of at least 24 repeats of the MS2-binding stem loop [10, 53–55]. When these loops (which each bind two MS2 proteins) are fully populated, a complex of more than 2,000 kilodaltons is produced. Such a structure is several times larger than most mRNA, giving the potential to perturb normal cellular behaviors. Riboglow reduces the size of the fluorescent probe by 10–100-fold (relative to the MS2 system), however, *recent data has shown that 12 copies of Riboglow linked in series are still necessary for single molecule resolution*.

With the wide variety of new probe constructs developed to reduce fluorescence background (Aim 1), changes will be made to the sequence of the cobalamin riboswitch *to further improve brightness to enable single molecule imaging with a single Riboglow copy*. *A directed evolution screen for fluorescence brightness will identify optimal riboswitch sequences that promote fluorescence signal induction*.

First, a library will be designed that varies the environment surrounding the cobalamin binding pocket (Figure 3A). Through the guidance of Robert Batey (see Batey support letter), sites will be chosen to retain affinity for the cobalamin, yet maximize the distance between quencher and fluorophore upon binding [5]. Next, a screen for fluorescence intensity in mammalian cells will be used to select bright riboswitch sequences (Figure 3B). A cellular screen for brightness is crucial because it ensures that the riboswitch aptamer maintains robust folding in a complex environment. The Palmer lab is a leader in technologies for tool development in mammalian cells [56, 57]. Libraries of transcripts will first be transduced into mammalian cells using lentivirus at a low multiplicity of infection to ensure incorporation of a single library member per cell (a technique widely used in the Palmer lab). The probe of interest will be administered, and cells will be sorted via fluorescence activated cell sorting (FACS, see Equipment document). Cells that show elevated brightness relative to a fluorescent protein expression control will be binned. In this way, libraries of up to one million members will be screened. I will collect, culture, and resubject bright variants to sorting until only highly fluorescent cells remain. Sequences will be evaluated through high-throughput sequencing.

New sequences identified through this screen will undergo rigorous characterization of their biophysical and photophysical properties *in vitro*. It will be important to characterize the extinction coefficient of each complex upon binding the RNA tag, as well as their quantum yields and photostability. The binding affinity for each probe-RNA combination will also be measured via isothermal titration calorimetry. Experiments to obtain these values are readily carried out in the Palmer Lab [4, 58]. I will aim to retain K_D values in the nanomolar range (optimal native riboswitches bind Riboglow probes at K_D = 3 nM). *Low K_D values will enable low substrate dosing (10-100 nM), further minimizing fluorescence background.*

Candidate probes that exhibit low background fluorescence, high signal induction, and high RNA affinity will be tested to determine the minimum number of fluorophores that can be localized. To do this, β-actin mRNA will be tagged with one, two, or four repeats of the mutant riboswitch of interest in U2-OS cells through transient transfection. The cells will be imaged under conditions analogous to previous studies [53] using a TIRF microscope (see Equipment document). If puncta that appear to be single molecules are observed under these conditions, probe localization will be verified via single-molecule fluorescence in situ hybridization (smFISH) following cell fixation [59]. This same method was recently used to quantify the sensitivity of an improved MS2 system [23].

If puncta are not visible in the initial TIRF images, cells will be treated with arsenite to induce the formation of stress granules (SGs) that also contain the protein G3BP1 [60–62]. G3BP1 can be tagged with the Halo-tag, and subsequently labeled with an orthogonal fluorophore to evaluate co-localization. This is a technique that the Palmer lab has previously used successfully to test Riboglow probes [4].

Expected Outcomes and alternate approaches:
To attain single-molecule resolution with Riboglow, the probes synthesized in Aim 1 will be screened with libraries of riboswitch mutants *in cellulo*, targeting at least a 12-fold improvement in fluorescence turn-on. Cells containing bright mutants will be sorted via FACS and analyzed. Library hits will be characterized *in vitro*, and tested via established assays for single-molecule localization *in cellulo*. While screening for high fluorescence in cells via FACS is the most efficient way to ensure robust turn-on, an alternative approach could involve alternating a screen for binding via *in vitro* selection (see Aim 3 for experimental detail) and in cellulo selection for fluorescence via FACS. If single-molecule resolution is not observed in the library hits, additional riboswitches (over the four repeats already planned) can also be added to concentrate fluorescent signal.

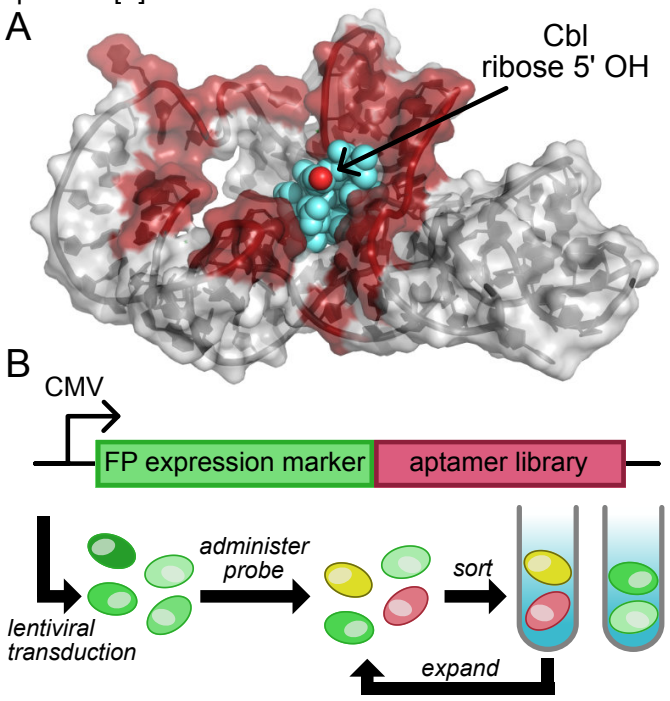

Figure 3. A) Riboswitch sites for mutation (colored red) will be targeted based on potential contact with the linker and fluorophore, while the cobalamin (blue) binding site will be retained. (PDB: 4FRN, ref. [5] B) RNA sequences will be screened in mammalian cells for brightness relative to a fluorescent protein control.

<u>Aim 3.</u> Develop mutually orthogonal Riboglow probes for multicomponent imaging.

The ability to track multiple RNA transcripts simultaneously would enable study of the interactions of RNA as they move throughout the cell. Upregulation of *SNHG5* in colorectal cancer has been implicated in stabilization of a variety of mRNA in the cytoplasm that enable tumor survival [16]. Direct hybridization of this lncRNA with mRNA protects transcipts from degradation, and enables translation, promoting disease states. Despite these implications, the spatiotemporal dynamics of lncRNA and their interacting partners have never been visualized in living cells, and thus their functions remain unknown. Localization of these lncRNA and their mRNA targets would shed light on these “dark” processes.

The modularity of the Riboglow platform is well suited to enable such an experiment, however mutually orthogonal riboswitch-probe pairs must first be identified *so that lncRNA and their interacting partners can both be tagged*. *In vitro selection will enable identification of mutually-selective riboswitch-probe pairs for multicomponent RNA imaging* (Figure 4B). *To start, I will identify two orthogonal riboglow probes.*

Fortunately, screening for substrate selectivity is well-precedented in RNA engineering through systematic evolution of ligands by exponential enrichment (SELEX) [63, 64]. In fact, *de novo* aptamers have already been developed for cobalamin and a few of its analogs via SELEX [65]. This important precedent shows that even small changes to the structure of the cobalamin can be distinguished by engineered RNA, indicating that no additional changes to the cobalamin structure may be necessary, apart from those constructs already proposed above.

Importantly, our selection experiments will not start from a completely randomized sequence of nucleic acids. It will be crucial to retain the original fold (and thus *in cellulo* stability) of the native riboswitch. RNA biosensors developed in this way are known to have increased stability relative to aptamers selected *de novo* [35]. Additionally, the brightest probe sequences identified in Aim 2 will be retained to preserve the bound conformation of the linker and fluorophore. The design of the starting RNA libraries, and subsequent selection experiments will be carried out under the supervision of Professor Robert Batey, an expert in SELEX and RNA engineering (see support letter) [35, 66]. Libraries will target bases known to participate in contacts with the cobalamin small molecule [5, 35]. The selection will be carried out as shown in Figure 4A. Briefly, the cobalamin probe of interest will be immobilized on a bead via the same linker that will be used in the final construct. The synthetic library of riboswitches will be incubated with the beads, and unbound sequences will be rinsed away. Riboswitches that bind selectively will be collected and amplified (via reverse transcription, PCR amplification, and transcription) to undergo another round of selection (for a total of 7-10 rounds). In subsequent rounds, the stringency of the screen will be increased via additional washes and reduction of RNA concentration. In the final 2-3 rounds of

selection, a counterselection will be conducted to ensure orthogonality with our other synthetic probes (Figure 4A). In this way, the probe (or probes) intended to be orthogonal to the construct under selection will wash away any riboswitches that do not bind selectively. Riboswitches will be deep sequenced to identify library convergence and optimal clones [35]. This process will be repeated for each probe of interest, with counterselections against each other probe that is intended for multiplexed use.

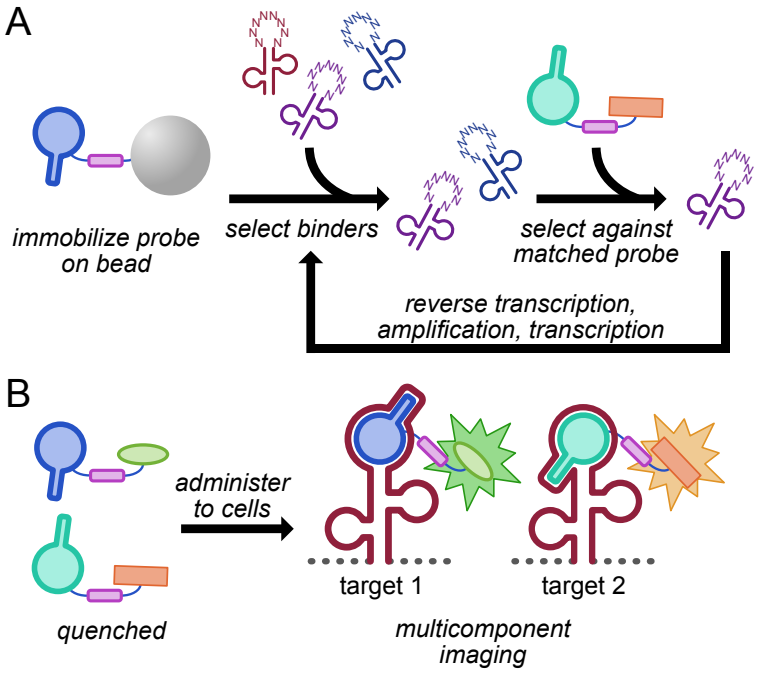

Figure 4. A) SELEX will be used to screen for riboswitches that bind each cobalamin in a mutually-exclusive manner. B) Mutually orthogonal cobalamin analogs will enable multicomponent RNA imaging. Signal turn-on will only be observed in the presence of the matched pair.

Mutually-orthogonal probes identified through the *in vitro* selection will be verified in a similar fashion as described in Aim 2. Probe extinction coefficient, quantum yield, photostability, and binding affinity will be characterized *in vitro*. Probes will also be independently verified *in cellulo* via the β-actin fusion assay described in Aim 2 to ensure signal induction was retained.

Once a robust pair of Riboglow probes is identified, a lncRNA will be imaged interacting with a putative binding partner mRNA. This proof-of-concept study will be conducted under the supervision of Professor John Rinn, an expert in lncRNA (see support letter). *For initial studies, we chose the lncRNA SNHG5. This 2 kilobase transcript is ideal because it localizes to the cytoplasm (where Riboglow concentration is likely highest), and has a variety of known interacting partners [16]. We are confident that lncRNA will be tolerant to Riboglow tagging because the MS2 system has previously been used to track lncRNA, employing four stem loops encoded downstream of the transcript of interest [67]. Additionally, SNHG5 has been tagged with the MS2 coat protein for RNA immunoprecipitation (RIP) without perturbing biosynthesis [18].* First, *SNHG5* will be tagged with one of our riboswitches and imaged in the cytosol of colorectal carcinoma (HCT116) cells, coupled with smFISH for verification. Known phenotypic checks will be used to ensure that *SNHG5* behaves normally upon tagging [16]. *If behavior is disrupted, alternate tag locations will be explored.*

Next, our multicomponent Riboglow platform will be used to image *SNHG5* interacting with known mRNA in the cytosol. *SNHG5* has been shown to promote colorectal cancer survival through base pairing in the 3'-UTR of mRNA that promote tumor growth [16]. *SPATS2*, *PTRM1*, and *GLE1* have been identified as interacting partners. To test whether these interactions can be detected, we will tag these three transcripts (one at a time) with an orthogonal riboswitch, and image them in living HCT116 cells alongside the tagged *SNHG5*. To further study these interactions, *SNHG5* will be both overexpressed (via transient expression) and knocked down (via RNA interference), which has been shown to increase and decrease, respectively, the levels of interacting transcripts [16]. An additional check for localization will be made through fluorescent tagging of *STAU1*, a protein that binds to the 3'-UTR of mRNA and mediates their degradation [68]. Single molecule FISH will provide a final check of probe selectivity.

Expected Outcomes and alternate approaches: To develop multicomponent Riboglow, *in vitro* selection will identify orthogonal riboswitch-probe pairs through a series of selections and counterselections. Following characterization *in vitro*, probes will be tested for multiplexed imaging of lncRNA-mRNA interactions *in cellulo*. It is possible that the *in vitro* selection will result in a loss of fluorescence turn-on. If this is the case, riboswitch sequences will be resubjected to the *in cellulo* fluorescence intensity screen described in Aim 2. Additionally, it may be difficult for the riboswitch to differentiate probes with similar cobalamin-linker structures. If the SELEX screen does not yield well-resolved pairs, additional steric bulk can be added to to the cobalamin (at either the 5' OH of the ribose, or the axial position of the cobalt), to aid in differentiation [36].

These studies will provide the first glimpse into the real-time behavior of lncRNA *SNHG5* and its interacting partners. With new tools in the RNA imaging toolkit, we will be able to ask new questions about lncRNA, the little-understood biomolecules that account for half of all cellular transcription [13, 14].

Bibliography and References Cited

[1] Cech, T. R. and Steitz, J. A.: The Noncoding RNA Revolution—Trashing Old Rules to Forge New Ones. Cell. 157(1): 77–94, March 2014.

[2] Müller-McNicoll, M. and Neugebauer, K. M.: How cells get the message: Dynamic assembly and function of mRNA–protein complexes. Nature Reviews Genetics. 14(4): 275–287, April 2013.

[3] Etzel, M. and Mörl, M.: Synthetic Riboswitches: From Plug and Pray toward Plug and Play. Biochemistry. 56(9): 1181–1198, March 2017.

[4] Braselmann, E., Wierzba, A. J., Polaski, J. T., Chromiński, M., Holmes, Z. E., Hung, S.-T., Batan, D., Wheeler, J. R., Parker, R., Jimenez, R., Gryko, D., Batey, R. T., and Palmer, A. E.: A multicolor riboswitch-based platform for imaging of RNA in live mammalian cells. Nature Chemical Biology. 1 pp, July 2018.

[5] Johnson Jr, J. E., Reyes, F. E., Polaski, J. T., and Batey, R. T.: B_{12} cofactors directly stabilize an mRNA regulatory switch. Nature. 492(7427): 133–137, December 2012.

[6] Paige, J. S., Wu, K. Y., and Jaffrey, S. R.: RNA Mimics of Green Fluorescent Protein. Science. 333(6042): 642–646, July 2011.

[7] Filonov, G. S., Moon, J. D., Svensen, N., and Jaffrey, S. R.: Broccoli: Rapid Selection of an RNA Mimic of Green Fluorescent Protein by Fluorescence-Based Selection and Directed Evolution. J. Am. Chem. Soc. 136(46): 16299–16308, November 2014.

[8] Autour, A., Jeng, S., Cawte, A., Abdolahzadeh, A., Galli, A., Panchapakesan, S. S. S., Rueda, D., Ryckelynck, M., and Unrau, P. J.: Fluorogenic RNA Mango aptamers for imaging small non-coding RNAs in mammalian cells. Nature Communications. 9(1): 656, February 2018.

[9] Dolgosheina, E. V., Jeng, S. C. Y., Panchapakesan, S. S. S., Cojocaru, R., Chen, P. S. K., Wilson, P. D., Hawkins, N., Wiggins, P. A., and Unrau, P. J.: RNA Mango Aptamer-Fluorophore: A Bright, High-Affinity Complex for RNA Labeling and Tracking. ACS Chem. Biol. 9(10): 2412–2420, October 2014.

[10] Fusco, D., Accornero, N., Lavoie, B., Shenoy, S. M., Blanchard, J.-M., Singer, R. H., and Bertrand, E.: Single mRNA Molecules Demonstrate Probabilistic Movement in Living Mammalian Cells. Current Biology. 13(2): 161–167, January 2003.

[11] Della Ragione, F., Gagliardi, M., D'Esposito, M., and Matarazzo, M. R.: Non-coding RNAs in chromatin disease involving neurological defects. Front. Cell. Neurosci. 8, 2014.

[12] Anastasiadou, E., Jacob, L. S., and Slack, F. J.: Non-coding RNA networks in cancer. Nature Reviews Cancer. 18(1): 5–18, January 2018.

[13] Rinn, J. L. and Chang, H. Y.: Genome Regulation by Long Noncoding RNAs. Annual Review of Biochemistry. 81(1): 145–166, 2012.

[14] Rinn, J. L., Euskirchen, G., Bertone, P., Martone, R., Luscombe, N. M., Hartman, S., Harrison, P. M., Nelson, F. K., Miller, P., Gerstein, M., Weissman, S., and Snyder, M.: The transcriptional activity of human Chromosome 22. Genes Dev. 17(4): 529–540, February 2003.

[15] Tanaka Ritsuko, , Satoh Hitoshi, , Moriyama Masatsugu, , Satoh Kasumi, , Morishita Yasuyuki, , Yoshida Syouko, , Watanabe Toshiki, , Nakamura Yoshikazu, , and Mori Shigeo, : Intronic U50 small-nucleolar-RNA (snoRNA) host gene of no protein-coding potential is mapped at the chromosome breakpoint t(3;6)(q27;q15) of human B-cell lymphoma. Genes to Cells. 5(4): 277–287, December 2001.

[16] Damas, N. D., Marcatti, M., Côme, C., Christensen, L. L., Nielsen, M. M., Baumgartner, R., Gylling, H. M., Maglieri, G., Rundsten, C. F., Seemann, S. E., Rapin, N., Thézenas, S., Vang, S., Ørntoft, T., Andersen, C. L., Pedersen, J. S., and Lund, A. H.: *SNHG5* promotes colorectal cancer cell survival by counteracting STAU1-mediated mRNA destabilization. Nature Communications. 7: 13875, December 2016.

[17] Zhao, L., Guo, H., Zhou, B., Feng, J., Li, Y., Han, T., Liu, L., Li, L., Zhang, S., Liu, Y., Shi, J., and Zheng, D.: Long non-coding RNA SNHG5 suppresses gastric cancer progression by trapping MTA2 in the cytosol. Oncogene. 35(44): 5770–5780, November 2016.

[18] He, B., Bai, Y., Kang, W., Zhang, X., and Jiang, X.: LncRNA SNHG5 regulates imatinib resistance in chronic myeloid leukemia via acting as a CeRNA against MiR-205-5p. Am J Cancer Res. 7(8): 1704–1713, PMC5574942, August 2017.

[19] Yan, L., Wang, S., Li, Y., Tognetti, L., Tan, R., Zeng, K., Pianigiani, E., Mi, X., Li, H., Fimiani, M., and Rubegni, P.: SNHG5 promotes proliferation and induces apoptosis in melanoma by sponging miR-155. RSC Advances. 8(11): 6160–6168, 2018.

[20] Ma, Z., Xue, S., Zeng, B., and Qiu, D.: lncRNA SNHG5 is associated with poor prognosis of bladder cancer and promotes bladder cancer cell proliferation through targeting p27. Oncology Letters. 15(2): 1924–1930, February 2018.

[21] Shen, H., Wang, Y., Shi, W., Sun, G., Hong, L., and Zhang, Y.: LncRNA SNHG5/miR-26a/SOX2 signal axis enhances proliferation of chondrocyte in osteoarthritis. Acta Biochim Biophys Sin (Shanghai). 50(2): 191–198, February 2018.

[22] Zheng, L., Hu, N., Guan, G., Chen, J., Zhou, X., and Li, M.: Long noncoding RNA SNHG6 promotes osteosarcoma cell proliferation through regulating p21 and KLF2. Archives of Biochemistry and Biophysics. Forthcoming 2018.

[23] Tutucci, E., Vera, M., Biswas, J., Garcia, J., Parker, R., and Singer, R. H.: An improved MS2 system for accurate reporting of the mRNA life cycle. Nature Methods. 15(1): 81–89, January 2018.

[24] Babendure, J. R., Adams, S. R., and Tsien, R. Y.: Aptamers Switch on Fluorescence of Triphenylmethane Dyes. J. Am. Chem. Soc. 125(48): 14716–14717, December 2003.

[25] Constantin, T. P., Silva, G. L., Robertson, K. L., Hamilton, T. P., Fague, K., Waggoner, A. S., and Armitage, B. A.: Synthesis of New Fluorogenic Cyanine Dyes and Incorporation into RNA Fluoromodules. Org. Lett. 10(8): 1561–1564, April 2008.

[26] Iii, R. J. T., Demeshkina, N. A., Lau, M. W. L., Panchapakesan, S. S. S., Jeng, S. C. Y., Unrau, P. J., and Ferré-D'Amaré, A. R.: Structural basis for high-affinity fluorophore binding and activation by RNA Mango. Nature Chemical Biology. 13(7): 807–813, July 2017.

[27] Warner, K. D., Chen, M. C., Song, W., Strack, R. L., Thorn, A., Jaffrey, S. R., and Ferré-D'Amaré, A. R.: Structural basis for activity of highly efficient RNA mimics of green fluorescent protein. Nature Structural & Molecular Biology. 21(8): 658–663, August 2014.

[28] Jeng, S. C. Y., Chan, H. H. Y., Booy, E. P., McKenna, S. A., and Unrau, P. J.: Fluorophore ligand binding and complex stabilization of the RNA Mango and RNA Spinach aptamers. RNA. 22(12): 1884–1892, January 2016.

[29] Morisaki, T., Lyon, K., DeLuca, K. F., DeLuca, J. G., English, B. P., Zhang, Z., Lavis, L. D., Grimm, J. B., Viswanathan, S., Looger, L. L., Lionnet, T., and Stasevich, T. J.: Real-time quantification of single RNA translation dynamics in living cells. Science. 352(6292): 1425–1429, June 2016.

[30] McNeil, P. L. and Warder, E.: Glass beads load macromolecules into living cells. Journal of Cell Science. 88(5): 669–678, December 1987.

[31] Hayashi-Takanaka, Y., Yamagata, K., Wakayama, T., Stasevich, T. J., Kainuma, T., Tsurimoto, T., Tachibana, M., Shinkai, Y., Kurumizaka, H., Nozaki, N., and Kimura, H.: Tracking epigenetic histone modifications in single cells using Fab-based live endogenous modification labeling. Nucleic Acids Res. 39(15): 6475–6488, August 2011.

[32] Rosendahl, M. S., Omann, G. M., and Leonard, N. J.: Synthesis and biological activity of a profluorescent analogue of coenzyme B12. PNAS. 79(11): 3480–3484, June 1982.

[33] Lee, M. and Grissom, C. B.: Design, Synthesis, and Characterization of Fluorescent Cobalamin Analogues with High Quantum Efficiencies. Org. Lett. 11(12): 2499–2502, June 2009.

[34] Smeltzer, C. C., Cannon, M. J., Pinson, P. R., Munger, J. D., West, F. G., and Grissom, C. B.: Synthesis and Characterization of Fluorescent Cobalamin (CobalaFluor) Derivatives for Imaging. Org. Lett. 3(6): 799–801, March 2001.

[35] Porter, E. B., Polaski, J. T., Morck, M. M., and Batey, R. T.: Recurrent RNA motifs as scaffolds for genetically encodable small-molecule biosensors. Nature Chemical Biology. 13(3): 295–301, March 2017.

[36] Chromiński, M., Lewalska, A., Karczewski, M., and Gryko, D.: Vitamin B12 Derivatives for Orthogonal Functionalization. J. Org. Chem. 79(16): 7532–7542, August 2014.

[37] Fesinmeyer, R. M., Hudson, F. M., and Andersen, N. H.: Enhanced Hairpin Stability through Loop Design: The Case of the Protein G B1 Domain Hairpin. J. Am. Chem. Soc. 126(23): 7238–7243, June 2004.

[38] Shell, T. A. and Lawrence, D. S.: Vitamin B12: A Tunable, Long Wavelength, Light-Responsive Platform for Launching Therapeutic Agents. Acc. Chem. Res. 48(11): 2866–2874, November 2015.

[39] Shell, T. A., Shell, J. R., Rodgers, Z. L., and Lawrence, D. S.: Tunable Visible and Near-IR Photoactivation of Light-Responsive Compounds by Using Fluorophores as Light-Capturing Antennas. Angewandte Chemie International Edition. 53(3): 875–878, January 2014.

[40] Cochran, A. G., Skelton, N. J., and Starovasnik, M. A.: Tryptophan zippers: Stable, monomeric β-hairpins. PNAS. 98(10): 5578–5583, May 2001.

[41] Kier, B. L. and Andersen, N. H.: Probing the Lower Size Limit for Protein-Like Fold Stability: Ten-Residue Microproteins With Specific, Rigid Structures in Water. J. Am. Chem. Soc. 130(44): 14675–14683, November 2008.

[42] Andersen, N. H., Olsen, K. A., Fesinmeyer, R. M., Tan, X., Hudson, F. M., Eidenschink, L. A., and Farazi, S. R.: Minimization and Optimization of Designed β-Hairpin Folds. J. Am. Chem. Soc. 128(18): 6101–6110, May 2006.

[43] Kolb Hartmuth C., , Finn M. G., , and Sharpless K. Barry, : Click Chemistry: Diverse Chemical Function from a Few Good Reactions. Angewandte Chemie International Edition. 40(11): 2004–2021, May 2001.

[44] Patterson, D. M., Nazarova, L. A., and Prescher, J. A.: Finding the Right (Bioorthogonal) Chemistry. ACS Chem. Biol. 9(3): 592–605, March 2014.

[45] Chromiński, M., Lewalska, A., and Gryko, D.: Reduction-free synthesis of stable acetylide cobalamins. Chemical Communications. 49(97): 11406–11408, 2013.

[46] Ruetz Markus, , Salchner Robert, , Wurst Klaus, , Fedosov Sergey, , and Kräutler Bernhard, : Phenylethynylcobalamin: A Light-Stable and Thermolysis-Resistant Organometallic Vitamin B12 Derivative Prepared by Radical Synthesis. Angewandte Chemie International Edition. 52(43): 11406–11409, September 2013.

[47] Pathare, P. M., Wilbur, D. S., Heusser, S., Quadros, E. V., McLoughlin, P., and Morgan, A. C.: Synthesis of Cobalamin-Biotin Conjugates That Vary in the Position of Cobalamin Coupling. Evaluation of Cobalamin Derivative Binding to Transcobalamin II. Bioconjugate Chem. 7(2): 217–232, January 1996.

[48] Grimm, J. B., Muthusamy, A. K., Liang, Y., Brown, T. A., Lemon, W. C., Patel, R., Lu, R., Macklin, J. J., Keller, P. J., Ji, N., and Lavis, L. D.: A general method to fine-tune fluorophores for live-cell and *in vivo* imaging. Nature Methods. 14(10): 987–994, October 2017.

[49] Grimm, J. B., English, B. P., Chen, J., Slaughter, J. P., Zhang, Z., Revyakin, A., Patel, R., Macklin, J. J., Normanno, D., Singer, R. H., Lionnet, T., and Lavis, L. D.: A general method to improve fluorophores for live-cell and single-molecule microscopy. Nature Methods. 12(3): 244–250, March 2015.

[50] Li, G.-W. and Xie, X. S.: Central dogma at the single-molecule level in living cells. Nature. 475(7356): 308–315, July 2011.

[51] Cabili, M. N., Dunagin, M. C., McClanahan, P. D., Biaesch, A., Padovan-Merhar, O., Regev, A., Rinn, J. L., and Raj, A.: Localization and abundance analysis of human lncRNAs at single-cell and single-molecule resolution. Genome Biology. 16: 20, January 2015.

[52] Andrecka, J., Lewis, R., Brückner, F., Lehmann, E., Cramer, P., and Michaelis, J.: Single-molecule tracking of mRNA exiting from RNA polymerase II. PNAS. 105(1): 135–140, January 2008.

[53] Katz, Z. B., English, B. P., Lionnet, T., Yoon, Y. J., Monnier, N., Ovryn, B., Bathe, M., and Singer, R. H.: Mapping translation 'hot-spots' in live cells by tracking single molecules of mRNA and ribosomes. eLife Sciences. 5: e10415, January 2016.

[54] Yamagishi, M., Ishihama, Y., Shirasaki, Y., Kurama, H., and Funatsu, T.: Single-molecule imaging of β-actin mRNAs in the cytoplasm of a living cell. Experimental Cell Research. 315(7): 1142–1147, April 2009.

[55] Halstead, J. M., Lionnet, T., Wilbertz, J. H., Wippich, F., Ephrussi, A., Singer, R. H., and Chao, J. A.: An RNA biosensor for imaging the first round of translation from single cells to living animals. Science. 347(6228): 1367–1671, March 2015.

[56] Fiedler, B. L., Van Buskirk, S., Carter, K. P., Qin, Y., Carpenter, M. C., Palmer, A. E., and Jimenez, R.: Droplet Microfluidic Flow Cytometer For Sorting On Transient Cellular Responses Of Genetically-Encoded Sensors. Anal. Chem. 89(1): 711–719, January 2017.

[57] Dean, K. M., Davis, L. M., Lubbeck, J. L., Manna, P., Friis, P., Palmer, A. E., and Jimenez, R.: High-Speed Multiparameter Photophysical Analyses of Fluorophore Libraries. Anal. Chem. 87(10): 5026–5030, May 2015.

[58] Park, J. G. and Palmer, A. E. Quantitative Measurement of Ca^{2+} and Zn^{2+} in Mammalian Cells Using Genetically Encoded Fluorescent Biosensors. In Fluorescent Protein-Based Biosensors, Methods in Molecular Biology, pp 29–47. Humana Press, Totowa, NJ, 2014.

[59] Mueller, F., Senecal, A., Tantale, K., Marie-Nelly, H., Ly, N., Collin, O., Basyuk, E., Bertrand, E., Darzacq, X., and Zimmer, C.: FISH-quant: Automatic counting of transcripts in 3D FISH images. Nature Methods. 10(4): 277–278, April 2013.

[60] Zurla, C., Lifland, A. W., and Santangelo, P. J.: Characterizing mRNA Interactions with RNA Granules during Translation Initiation Inhibition. PLOS ONE. 6(5): e19727, May 2011.

[61] Jain, S., Wheeler, J. R., Walters, R. W., Agrawal, A., Barsic, A., and Parker, R.: ATPase-Modulated Stress Granules Contain a Diverse Proteome and Substructure. Cell. 164(3): 487–498, January 2016.

[62] Nelles, D. A., Fang, M. Y., O'Connell, M. R., Xu, J. L., Markmiller, S. J., Doudna, J. A., and Yeo, G. W.: Programmable RNA Tracking in Live Cells with CRISPR/Cas9. Cell. 165(2): 488–496, April 2016.

[63] Mairal, T., Özalp, V. C., Sánchez, P. L., Mir, M., Katakis, I., and O'Sullivan, C. K.: Aptamers: Molecular tools for analytical applications. Anal Bioanal Chem. 390(4): 989–1007, February 2008.

[64] Cho, E. J., Lee, J.-W., and Ellington, A. D.: Applications of Aptamers as Sensors. Annual Review of Analytical Chemistry. 2(1): 241–264, 2009.

[65] Lorsch, J. R. and Szostak, J. W.: In vitro selection of RNA aptamers specific for cyanocobalamin. Biochemistry. 33(4): 973–982, February 1994.

[66] Trausch, J. J. and Batey, R. T. Chapter Three - Design of Modular "Plug-and-Play" Expression Platforms Derived from Natural Riboswitches for Engineering Novel Genetically Encodable RNA Regulatory Devices. In Burke-Aguero, D. H. (Ed.): Methods in Enzymology, volume 550 of *Riboswitches as Targets and Tools*, pp 41–71. Academic Press, January 2015.

[67] Yoon, J.-H., Abdelmohsen, K., Srikantan, S., Yang, X., Martindale, J. L., De, S., Huarte, M., Zhan, M., Becker, K. G., and Gorospe, M.: LincRNA-p21 Suppresses Target mRNA Translation. Molecular Cell. 47(4): 648–655, August 2012.

[68] Park Eonyoung, and Maquat Lynne E., : Staufen-mediated mRNA decay. Wiley Interdisciplinary Reviews: RNA. 4(4): 423–435, June 2013.